Fisheries Research 244 (2021) 106117

Contents lists available at ScienceDirect

Fisheries Research

journal homepage: www.elsevier.com/locate/fishres

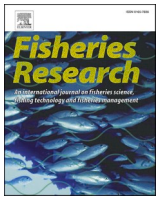

Full length article

Spatial and temporal patterns of capelin (*Mallotus villosus*) spawning sites in the Barents Sea

Salah Alrabeei [a,b,*], Sam Subbey [a,b], Sofie Gundersen [b], Harald Gjøsæter [b]

[a] Western Norway University of Applied Sciences, Bergen, Norway
[b] Institute of Marine Research, Bergen, Norway

ARTICLE INFO

Handled by: Prof. George A. Rose

Keywords:
Capelin
Barents Sea
Spawning sites
Clustering analysis

ABSTRACT

Identifying spawning sites of fish often involves extensive egg and larval sampling surveys over potential spawning sites, or by backward-tracking advected larvae to their source. Due to the vastness of the Barents Sea capelin spawning areas, back-tracking methods have limited application. Egg and larval surveys that provide information about spawning sites have also been discontinued in recent years. This paper aims at using alternative data sources to egg and larval distribution information, to infer potential spawning regions of the Barents Sea capelin during the period 1994–2020. We use the K-Means clustering technique to cluster historical spawning sites into spawning regions, and the Self Organizing Map (SOM) algorithm to define observed data clusters, which we assign to specific regions. The observation data consists of survey data sets from capelin pre-spawning and post-spawning periods during winter and spring respectively, as well as data from the Norwegian Directorate of Fisheries Electronic Reporting System database (ERS). Our method was efficient in reproducing capelin spawning regions and approximate time windows for commencement of spawning. The results showed that spawning occurred mainly over the eastern part of historical spawning areas during the whole period. A westward extension of the preferred spawning areas occurred in several years regardless of the rising Barents Sea water temperatures, especially during the second half of the period. The ERS data can be used to identify the arrival times and migration fronts of pre-spawning capelin along the coast.

1. Introduction

Knowledge of when fish spawn and the spatial location where spawning activities occur are central to fisheries ecology, conservation, and management. Some species, such as capelin (*Mallotus villosus*), spawn only once in their life-cycle (Christiansen et al., 2008) and are often short-lived. The commercial exploitation of short-lived species is often managed by a so-called spawning escapement strategy, where the aim of the management is to allow a sufficient amount of spawners to escape the fishery to secure adequate recruitment. This strategy is applied to the Barents Sea capelin stock (Gjøsæter et al., 2002), and the timing and level of the fisheries must be such that it is not detrimental to the spawning activity. Recruitment failure may occur when the combination of timing and localization of the spots of commercial fisheries result in a reduction of the population of potential spawners to low-density threshold levels (Sadovy and Domeier, 2005). Identifying when and where the spawning occurs could help to define accurate spatial and temporal ranges of dedicated surveys to quantify the size of the spawning stock, or in establishing marine protected areas (MPAs). Moreover, this knowledge could help establish a relationship between spawning areas and spawning success. Such a relationship might be useful for the first assessment of recruitment potential after spawning (Gjøsæter, 1972). The spawning grounds for migratory fish are usually assumed to be fixed as these sites, through an interaction between their geomorphological and oceanographic conditions, represent optimal locations for the survival of the offspring (Bauer et al., 2014). Hence, the timing of spawning activity and spawning sites may change over time, as an adaptation to changes in environmental conditions (Erisman et al., 2017; Petitgas et al., 2010). However, considering a short-lived semelparous species, adaptation through social learning is not possible while a homing instinct, possibly in combination with a direct reaction to the environment or indirect reaction due to the environment's effect on timing of maturation are more likely mechanisms. That is, fish have a genetic trait to partially determine where and when to spawn, but the choice of spawning area each year is adapted to the environmental conditions during the pre-spawning period.

* Corresponding author at: Western Norway University of Applied Sciences, Bergen, Norway.
E-mail address: salah.alrabeei@hvl.no (S. Alrabeei).

https://doi.org/10.1016/j.fishres.2021.106117
Received 16 March 2021; Received in revised form 15 August 2021; Accepted 20 August 2021
Available online 4 September 2021

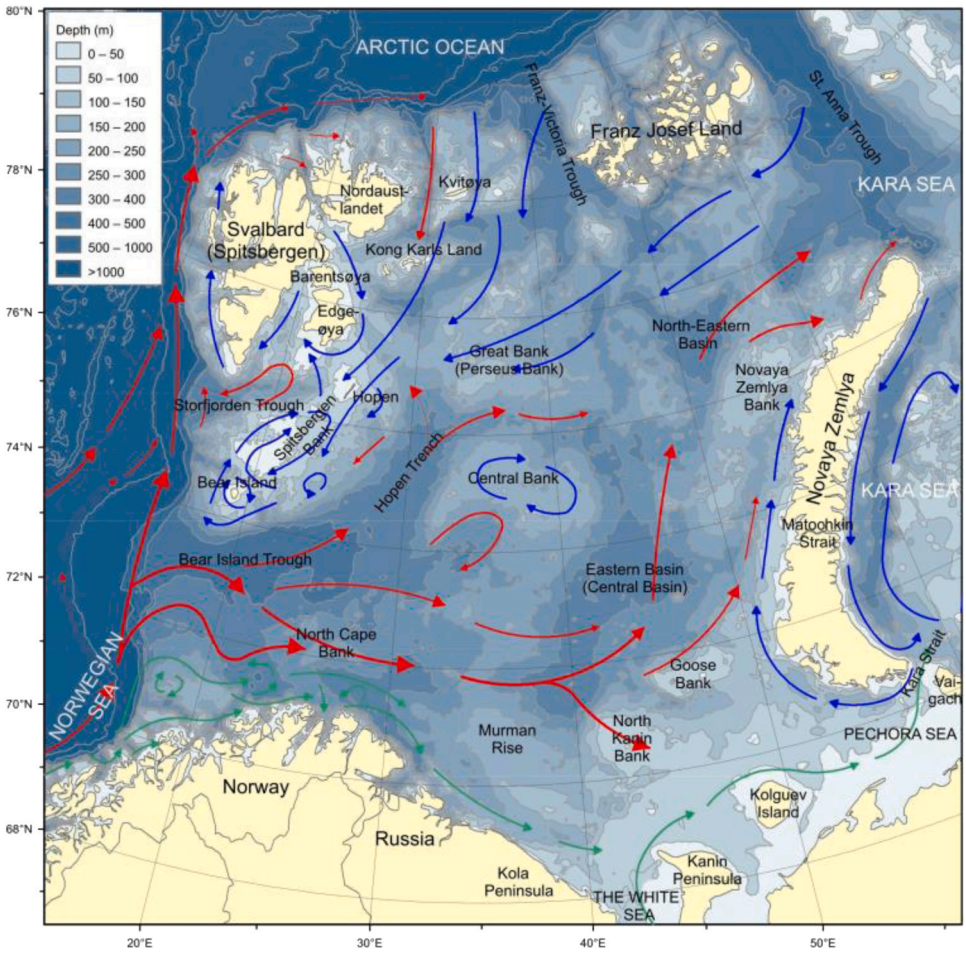

Fig. 1. The Barents Sea. Red arrows show Atlantic water currents, blue arrows Arctic currents, and green arrows currents of coastal waters. Used with courtesy of the Institute of Marine Research, Norway. (For interpretation of the references to colour in this figure legend, the reader is referred to the web version of this article.)

The Barents Sea is a high-latitude shelf sea bounded in the north and west by the continental edge towards the deep Arctic Ocean (at about 80–81°N) and the Norwegian Sea (at about 10–15°E) (Carmack et al., 2006). The oceanographic conditions of the Barents Sea are characterized by three water masses flowing into it; Atlantic, coastal, and Arctic waters (Fig. 1) (Loeng, 1991; Ingvaldsen and Gjøsæter, 2013). These conditions greatly affect the locations of the spawning, nursery, and feeding areas of the species inhabiting the Barents Sea, such as capelin (Ushakov and Ozhigin, 1987; Gjøsæter, 1998).

Barents Sea capelin, hereafter referred to as capelin, is a small pelagic, schooling fish that inhabits the Barents Sea during all life stages (Gjøsæter, 1998; Carscadden et al., 2013b). It undertakes extensive seasonal migrations throughout its lifetime. During winter and early spring, the mature individuals migrate from their overwintering areas in the central Barents Sea towards the spawning grounds near the coasts of northern Norway (Troms and Finnmark county) and Russia (Kola peninsula) (Fig. 2). After laying their eggs on the spawning grounds, most of the capelin die (Christiansen et al., 2008). The eggs hatch after about one month, and the larvae ascend to the upper water masses and are transported offshore, carried by the ocean currents towards capelin nursery regions occupying the central and eastern Barents Sea (Gjøsæter, 1998). During winter, the immature capelin move slightly southward from the area of overwintering to feed on the spring bloom, which occurs earlier over the coastal banks than over deeper ocean further offshore. Later, when the ice starts to melt, the adult capelin migrate northwards to feed on the blooming zooplankton (Gjøsæter, 1998).

Ozhigin and Luka (1985)) and Huse and Ellingsen (2008)) both showed that capelin annual migration pattern is determined by environmental factors such as the water temperature and capelin food density. All populations of this short-lived semelparous species have displayed a similar lack of tradition in habitat-use patterns (Petitgas et al., 2010). A first step in determining which environmental variables dictate the choice of spawning site, however, is premised on mapping out the migration routes and their end-points, which serve as spots for spawning activity.

A period of intensive studies of the capelin was initiated in late 1960, motivated by a major shift in the Norwegian pelagic fisheries from stocks of herring and mackerel in the North- and Norwegian Seas, which dwindled from the mid-1960s, to capelin, which was a previously almost unexploited resource (Hamre, 1985). Several annual studies were conducted during the period 1970–1990 to investigate where and when capelin was spawning and the geographical distribution and abundance of larvae in summer and autumn (Monstad and Midttun, 1973; Hamre and Sætre, 1976; Dommasnes and Hamre, 1977; Alvheim et al., 1983). Furthermore, short-term (Dragesund et al., 1973; Sætre and Gjøsæter, 1975; Loeng et al., 1983) and long-term reviews (Ozhigin and Ushakov, 1985; Gjøsæter, 1998, and references therein) have been conducted to investigate timing and sites of capelin spawning. These reviews show that the large-scale temperature variation, which has occurred since the mid-1970 s, has directly and indirectly affected the spawning migration and choice of spawning grounds (Ozhigin and Luka, 1985; Ozhigin and Ushakov, 1985).

Identifying the spawning areas of the capelin remains a challenge due to the large area of the main spawning sites – varying from off the western Troms region to East Finnmark or some years even to the coast of the Kola peninsula (Gjøsæter, 1998; Skaret et al., 2020) – and the variable arrival times for fish scheduled to spawn. A combination of

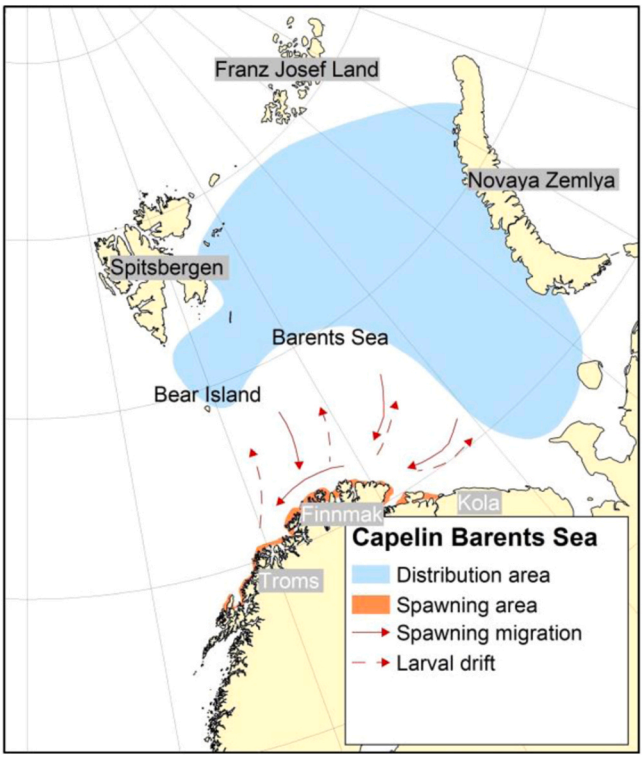

Fig. 2. Capelin grounds in the Barents Sea. Used with courtesy of the Institute of Marine Research, Norway.

Table 1
The primary data sources and their purpose used in this paper: Larval Survey (LS), Winter Survey (WS), and ERS data (ERS).

Data source	Years	Purpose
LS	1982–1985[a]	For testing and validation
	1988–1993	
WS and LS	1994–2006	For prediction
WS	2007–2010	
	2016–2017	
	2019–2020	
WS and ERS	2011–2015	
	2018	

[a] The capelin experienced a stock collapse during the period (1982–1993). Therefore, we chose to exclude 1986 and 1987 from our dataset, as we did not have sufficient data from these two years

direct and indirect observational methods have been used by the Institute of Marine Research (IMR) to identify the location of capelin spawning grounds, such as monitoring capelin landings in the near-shore fisheries (Gjøsæter, 1972), monitoring the migrating maturing capelin by acoustic surveys, and sampling the stomach contents of demersal fishes feeding on capelin eggs (e.g., cod and haddock) (Sætre and Gjøsæter, 1975). Recorded concentrations of diving ducks feeding on capelin eggs were used to limit the most likely spawning areas, capelin egg sampling with Petersens grab and underwater diving (SCUBA) methods were used to confirm and give more details on capelin spawning grounds and timing. Furthermore, capelin larval surveys were used to confirm that all spawning grounds had been found (Gjøsæter et al., 1972; Bakke and Bjørke, 1973; Sætre and Gjøsæter, 1975; Gjøsæter, 1998). However, due to the large area of investigation, which requires large resources for surveying, some of these efficient methods were discontinued; egg sampling with Petersens grab method was discontinued in 1984 which, was the essential method to determine the spawning locations (Gjøsæter, 1998). For the same reason, the capelin larval survey was discontinued in 2006 (Carscadden et al., 2013a) limiting the use of particle-tracking modeling to track backward in time the advected larvae to their source (spawning sites) (Bidegain et al., 2013; Bauer et al., 2014; Kvile et al., 2017).

In this paper, we integrate information and evidence from scientific surveys in winter, capelin larval spring surveys, and the Norwegian Directorate of Fisheries Electronic Reporting System (ERS) observations in winter to reconstruct spawning areas of capelin during the years 1994–2020. Furthermore, we investigate the ability to estimate the capelin spawning time using the ERS observations when available. This period has witnessed several episodes of collapse in the capelin stock, and the highest variability in water temperature ever recorded in the Barents Sea (ICES, 2019). ERS data have been used in several studies to describe fish spawning behavior (Carscadden et al., 1997; Vitale et al., 2008; Erisman et al., 2012; Tobin et al., 2013). Such data have recently been used to assess the timing and spawning migration route of the Icelandic capelin (Singh et al., 2020). Since the ERS data cover most of the spawning season and most of the potential spawning area, these data may give a more detailed description of the spatial and temporal development of the spawning activities. A challenge to our approach is the large spatial extent of potential spawning sites and modest resolution of the observation data, which limit our ability to identify variability in the choice of specific spawning sites. We are also limited by the lack of essential scientific survey data due to the discontinuation of the surveys as explained previously, during the period 2007–2020. As we show later in this paper, we address these challenges through several steps. Instead of spawning sites, we define contiguous spawning regions through coarse-graining of historically identified spawning sites. This paper aims to reproduce capelin spawning regions during the period 1994–2020 and inform variability in timing and spawning locations by analyzing capelin spatial distribution before and after the spawning activities.

2. Materials and methods

2.1. Data sources and data preprocessing

The analysis in the present paper is based on both fishery-independent and fishery-dependent data sources. The fishery-independent data include data from a joint Norwegian-Russian survey performed by the Norwegian Institute of Marine Research (IMR) and the Polar Branch of the Russian Federal Institute of Fisheries and Oceanography (VNIRO formerly PINRO). The winter survey (1981-) is executed annually from the end of January to the end of March, covering the south-central Barents Sea during the pre-spawning season of capelin when it undertakes its spawning migration (Mehl et al., 2014; Fall et al., 2020). It should be noted that this survey is designed as a trawl-acoustic survey targeting ground fish like cod and haddock, and the data obtained for capelin are therefore partly incomplete most years. We considered spatial locations and the number of mature capelin in each trawl catch. The mature capelin are characterized by having a length larger than 14 cm (Gjøsæter et al., 2016). Another fishery-independent source is a larval survey of capelin, which was conducted annually (1981–2006) in the first half of June, covering the southern Barents Sea (Alvheim, 1985; Eriksen, 2014). The IMR performed the survey to investigate the distribution and abundance of the larvae when most of the larvae are about one-month old (Gjøsæter, 1998).

The fishery-dependent data are collected by the Norwegian Directorate of Fisheries, and include data from the ERS from high-seas vessels above 15 m from (2011–2020) with exception of the periods 2016–2017 and 2019–2020, due to the moratorium on capelin fisheries. These data are used to locate the area where the fishermen intended to fish for capelin, where capelin was caught, and the abundance of the catches throughout the year. The data contain several species in each catch, and several locations along the Norwegian coast during the entire year. For our application, we only consider the catches that occurred during January-April, in which capelin were the target species. Only potential spawning capelin (mature) approach the coasts of the spawning regions where the fishery

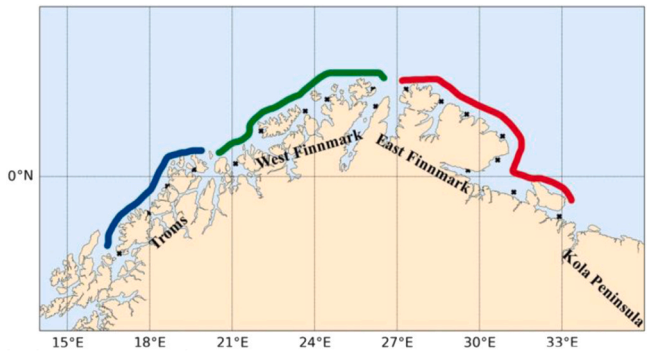

Fig. 3. Approximate capelin historical spawning sites (crosses) along the Norwegian coast categorized into three regions: Troms (blue line), West Finnmark (green line), and East Finnmark (red line). (For interpretation of the references to colour in this figure legend, the reader is referred to the web version of this article.)

activities (within the ERS spatial domain) take place. Hence filtering of the ERS data (using a 14 cm maturation cut-off) is not required.

For validating our method, results from the egg surveys and other information about where capelin spawning occurred in various years are summarized in Gjøsæter (1998).

In the present paper, the primary data covering the periods 1982–1993 and 1994–2020 were divided based on their availability and usage as in Table 1. The data sources were used evenly when more than one is available in the same year.

We characterize temperature variability in capelin spawning areas using time series of temperature at the Fugløya - Bjørnøya (FB) section, located at the southwestern Barents Sea. This section gives the temperature at depth intervals between 50 and 200 m of the inflowing Atlantic water (Ingvaldsen et al., 2003).

2.2. Methodological approach

Our approach can be summarized in the following three procedural steps:

1. Categorize the historical spawning sites into j non-overlapping spatial regions, $S^{(1)}$, …, $S^{(j)}$, each containing a finite number of spawning sites
2. Derive a maximum of N clusters, D_1, …, D_N of the capelin distribution data (given in (Table 1)) and their corresponding cluster centroids (or Center of Gravity – CoG) $\overline{P}_1, \ldots, \overline{P}_N$,
3. Assign data cluster D_j to spawning region $S^{(k)}$ if the relative sum of distances between $\overline{P}_j$ and all the spawning sites in $S^{(k)}$ is least when compared to similar numbers for all other spawning regions.

Details of the steps are discussed below.

2.2.1. Categorizing spawning sites

Capelin has historically spawned over several spawning sites scattered along the northern Norwegian coast. However, the available datasets limited our methodology to determine the spawning location on a finer scale (up to the spawning site). Therefore, we categorized the historical spawning sites into three spawning regions; Troms region between 16°E and 20°E, West Finnmark region between 20°E and 28°E, and East Finnmark region between 28°E and 32°E (Fig. 3). The number of spawning regions was chosen according to the maximum number of directions from which the spawning capelin approach the coast. The delineation of the three spawning regions was arbitrarily set to divide the total area into three regions.

2.2.2. Deriving capelin data clusters

We used a two-step approach in clustering the capelin distribution data (Table 1). In the first step, we used a Self-Organizing Map (SOM) (Kohonen, 1990) to generate $n \times m$ grid cells, defined over the data. In the second step, we applied the K-means (KM) clustering algorithm (Kanungo et al., 2002) to the grid cells from the SOM algorithm, to generate, at most, three data clusters. We used the 2-step approach in order to obtain as many initial candidates as possible in the first step (using SOM) and to reduce the candidates to three clusters (using the KM algorithm).

We used an approach based on representing a spatial distribution of data by its spatial mean, which is often referred to as the centroid or center of gravity (CoG) (Bez and Rivoirard, 2001; Woillez et al., 2009). We derived the CoGs as a weighted average of each dataset (catch) and its location, with weights representing the area of influence around the dataset. Let $k(\equiv \{1, \ldots, N_k\})$ represent the number of capelin stations sampled within a cluster, where each sample station has n_k number of caught capelin at location (Latitude,Longitude) $\boldsymbol{P}^k \equiv \{p_x^{(k)}, p_y^{(k)}\}$. Since the sampled grid is non-uniform, each station can be assumed to have a spatially defined area of influence a_k, which we defined later. The CoG of the N_k datasets, $\overline{\boldsymbol{P}} \equiv \{\overline{p}_x, \overline{p}_y\}$ is given by

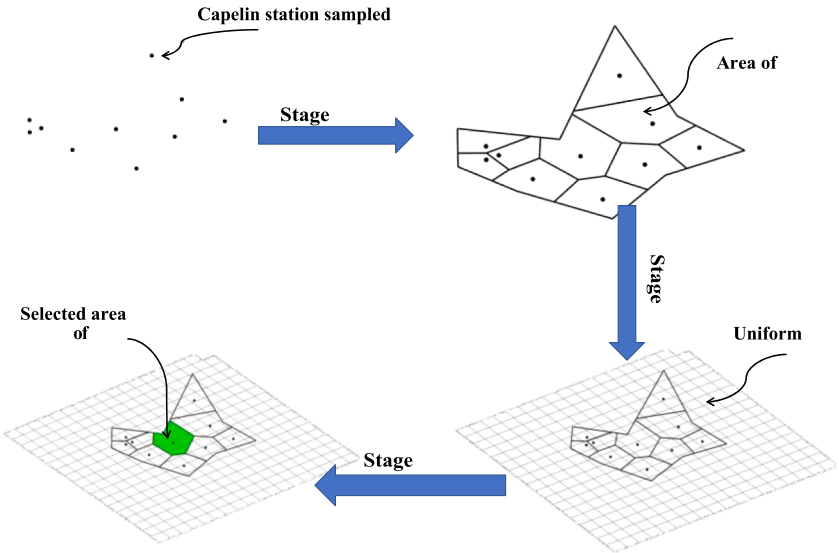

Fig. 4. Estimate the area of influence around each capelin sampled station. Stage one: Use Voronoi tessellation to define the area of influence over the whole domain. Stage two: generate finer and regular grids of area h^2 over the whole survey domain. Stage three: estimate the selected Voronoi cell by the total number (m_k) of uniform cells embedded in the Voronoi cell multiplied by the area of the uniform cell defined in stage two.

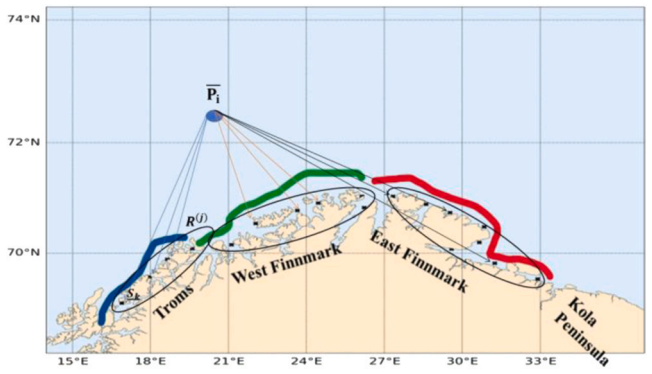

Fig. 5. For each spawning region $R^{(j)}$ (ellipses) (for $j = 1, 2, 3$), the distance (arrows) is calculated from each historical spawning site S_k (within the spawning region) to each CoG $\overline{P}_i$ for ($i = 1, \ldots, N$).

$$\overline{\boldsymbol{P}} \equiv \left(\overline{A} \sum_{k=1}^{N_k} n_k a_k p_x^{(k)}, \overline{A} \sum_{k=1}^{N_k} n_k a_k p_y^{(k)} \right); \quad \overline{A} = 1/\sum_{k=1}^{N_k} n_k a_k. \tag{1}$$

Defining the area of influence a_k

Given N_k points in a two-dimensional space Ω, the goal is to partition the space into $\Omega_1, \ldots, \Omega_{N_k}$ sub-domains, so that each point k has an area of influence $a_k = \Omega_k$. The simplest approach involves defining a Voronoi tessellation over Ω, and calculating the area of the Voronoi cell associated with point k. The Voronoi tessellation divides the plane according to the nearest neighbor rule; namely, each point is associated with the region of the plane closest to it. The distance metric is usually Euclidean, and each Voronoi polygon in the Voronoi diagram is defined by a generator point and the nearest neighbor region (Tanemura et al., 1983; Boots and Tiefelsdorf, 2000). Since the distribution of the samples (points) is not regular, the Voronoi tessellation has been considered as a more appropriate geometry to demarcate the area of influence than using uniform grid cells.

For the case where the domain has non-regular boundaries, such as in our case, calculating each Voronoi cell area is non-trivial. Hence we used a more pragmatic, two-step approach. In the first step, we defined a Voronoi tessellation over the Ω, to obtain N_k Voronoi cells. Next, we overlayed the Voronoi diagram with finely divided uniform grids over Ω, where the area of each fine grid is known (Fig. 4). Then a_k can be approximated by the sum of uniform grids embedded in Voronoi cell k, multiplied by the area of a uniform cell, i.e.,

$$a_k \approx m_k \overline{a}, \tag{2}$$

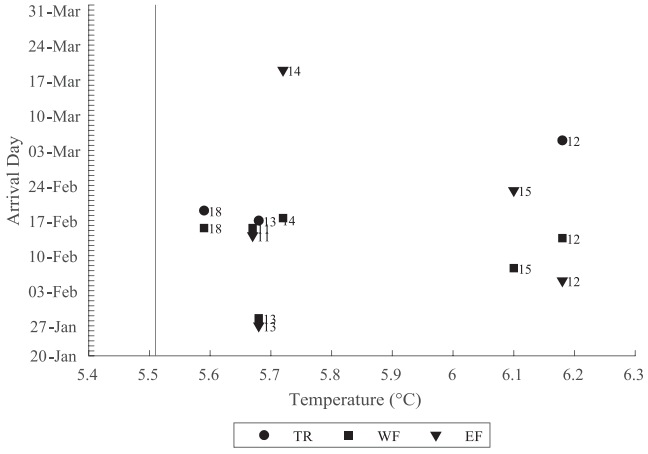

Fig. 6. Capelin arrival day and annual temperatures. The vertical line represents the average annual temperature (5.51 °C) in the Western Barents Sea from 1977 to 2019, at depth 50–200 m. The symbols represent capelin arrival time to the spawning regions Troms (TR), West Finnmark (WF), and East Finnmark (EF) in a given year (denoted by its last two digits), based on data from ERS.

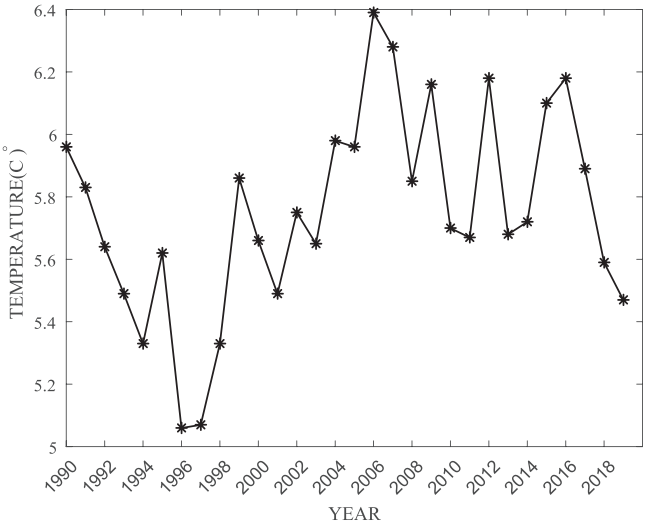

Fig. 7. Western Barents Sea annual temperature measured at depth 50–200 m at the degrees (20°E, 73°N). The average annual temperature of the period 1977–2019 is 5.51 °C.

Table 2
A comparison between capelin spawning occurrence status according to our method and according to the observational surveys (in parenthesis) described in Gjøsæter (1998)). The status:(1 = spawning occurred, 0 = no spawning occurred). The spawning regions: Troms region (TR), West Finnmark (WF), and East Finnmark (EF).

Year	1982	1983	1984	1985	1988	1989	1990	1991	1992	1993
TR	1(1)	1(1)	0(1)	1(1)	0(1)	1(1)	0(0)	1(1)	0(0)	0(0)
WF	1(1)	1(1)	1(1)	1(1)	1(1)	1(1)	1(1)	1(1)	1(1)	1(1)
EF	1(1)	1(1)	1(1)	1(1)	1(1)	1(1)	1(1)	1(1)	1(1)	1(1)

Table 3
Predicted capelin spawning occurrence (1 = spawning occurred, 0 = no spawning occurred) over the historical spawning regions (Troms (TR), West Finnmark (WF), and East Finnmark (EF)) during the period 1994–2020.

Year	1994	1995	1996	1997	1998	1999	2000	2001	2002	2003	2004	2005	2006
TR	0	1	1	0	0	0	1	0	0	1	1	0	1
WF	1	1	1	1	1	1	1	1	1	1	1	1	1
EF	1	1	1	1	1	1	1	1	1	1	1	1	1
Year	2007	2008	2009	2010	2011	2012	2013	2014	2015	2016	2017	2018	2019	2020
TR	1	1	1	0	0	1	1	0	0	1	1	1	0	1
WF	1	1	1	1	1	1	1	1	1	1	1	1	1	1
EF	1	1	1	1	1	1	1	1	1	1	1	1	1	1

where $\bar{a}$ is the area of a unit uniform cell, and m_k is the total number of uniform cells embedded in Voronoi cell k. Fig. 4 gives an illustrative example of the approach. Note that $\bar{a}$ cancels out, when (2) is substituted into (1). Hence, calculating $\overline{\boldsymbol{P}}$ only requires knowledge of the number of uniform grid cells encapsulated by each Voronoi cell.

2.2.3. Assignment of spawning region

The goal was to assign a capelin distribution to its nearest spawning region. The computational approach was divided into two steps. In the first step, for each categorized spawning region, we calculated the sum of distances between a given CoG (representing the data) and the spawning sites within the region. Next, we converted the sum of distances for each region into relative indices, and assigned the data (CoG) to the region with the least relative index (Fig. 5). The detailed computational procedure is described in the next paragraph.

Let $\mathscr{C} = \{\overline{\boldsymbol{P}}_1, \ldots, \overline{\boldsymbol{P}}_N\}$ represent the complete set of N CoG calculated using (1). Furthermore, assume that each spawning region $R^{(j)}$ ($j = 1, 2, 3$), is associated with $\mathscr{S}^{(j)} = \{S_1, \ldots, S_{n_j}\}$ spawning sites, where the value of n_j is determined by the specific spawning region of interest. Then for each spawning region $R^{(j)}$, we calculated the $n_j \times N$ matrix $\mathbf{D}$, which measures the Euclidean distance between each element of $\mathscr{C}$ and $\mathscr{S}^{(j)}$, and a row vector of indices $M^{(j)}$ defined by (3), where in general $\mathbf{I}_\kappa$ is a column vector with κ entries that are all 1′s, and $\mathbf{I}_\kappa^T$ is the transpose of $\mathbf{I}_\kappa$. Note that any arbitrary column $i \leq N$ in (3) is the average sum of Euclidean distances from $\overline{\boldsymbol{P}}_i$ to all the spawning sites in $R^{(j)}$. Finally, we formed the $3 \times N$ relative distance matrix $\mathbf{R}$, whose elements, $r_{j,i}$, $i = 1, \ldots, N$ are given by (4).

$$M^{(j)} = \frac{1}{n_j}\mathbf{I}_{n_j}^T \cdot \mathbf{D}, \tag{3}$$

$$r_{j,i} = M^{(j)}(i) / \sum_{j=1}^{3} \mathrm{M}^{(j)}(\mathrm{i}) \tag{4}$$

For each i (column), we identified the row, $j_m \leq 3$ with the least value of $r_{j,i}$ (i.e., relatively nearest spawning region). We assigned $\overline{\boldsymbol{P}}_i$ to spawning region j_m.

3. Results

For the ten years (1982–1985 and 1988–1993) used to test our method, results show high accuracy in determining capelin spawning regions (Table 2).

As our method showed high accuracy to reproduce the observed capelin spawning regions, we applied the method for the period after 1993, where we had no knowledge of where the capelin spawned. The results showed that in the last three decades (1993–2020), capelin has mainly spawned off the coast of Finnmark. The spawning regions extended towards the coast of Troms in several years (almost half of the period). Most of the western spawning (over Troms) occurred in the second half of the period (Table 3). However, the spatial distribution of the spawning sites within each predicted spawning region varies between years (Figs. A.1-A.4).

Using ERS data, the arrival time (in days) of the spawning capelin at each spawning region is approximated. In most of the years, capelin approached the coast of the spawning regions in the first two weeks of February, with an exception in 2013, when the capelin arrived earlier, i.e., in late January (Fig. 6).

4. Discussion

This study is motivated by a desire to increase our knowledge of how the distribution of capelin spawning sites has changed in the last three decades. This period has witnessed several episodes of collapse in the capelin stock and the highest variability in water temperature ever recorded in the Barents Sea (ICES, 2019). As the capelin spawning sites for the period (early 1960s - early 1990s) are described in Gjøsæter (1998)) based on direct observational surveys, we wanted to extend this long-term knowledge on capelin spawning sites up to the recent years. However, since the surveys used in Gjøsæter (1998)) have been discontinued, we could not use the same data sources for the period after 1994. Therefore, we used different data sources to test and validate our method, and then predict the spawning sites.

Our method showed high accuracy in determining capelin spawning regions when compared with those observed. It was only in the Troms region our method failed to describe the spawning occurrence in the years 1984 and 1988 correctly. A possible explanation is that our method depends solely on the larval survey data during the period 1982–1993. There could have been spawning outside Troms in 1984, but the larvae were advected by the coastal current eastward, and may therefore not have been captured by the survey off the coast of Troms. As a result, our method could not capture the spawning outside Troms.

Integrating different capelin spatial distributions during the pre-spawning and post-spawning periods allowed us to approximately locate the spawning sites and the approximate timing of the spawning activity within each spawning region. Capelin spawning sites were distributed mainly over the coast of Finnmark during the period 1994–2020. Spawning outside Troms occurred only in some years of the period. Based on our investigated time series (1994–2020), there was no obvious distributional shift of capelin larval or mature capelin over year that could be linked to the predicted westward shift of spawning areas.

According to the literature (Ozhigin and Ushakov, 1985; Gjøsæter, 1998; Carscadden et al., 1997), capelin spawning site selection is determined by hydrographic factors such as, the water temperature before and during the migration. That is, in warmer years – characterized by a strong inflow of Atlantic water from the west and high temperatures in the west (Fig. 7)- capelin spawning takes place over the spawning sites along the coast of Finnmark while in colder years, the spawning sites are extended westward to the west coast of the Troms region. However, our results do not appear to be consistent with the literature. For example, in 2006–2007 and 2012, capelin spawned over the coast of Troms region although the water temperature was higher than normal (Fig. 7). On the other hand, no spawning activity was registered in the Troms region during the low temperature registered in 2019 (Skaret et al., 2020). Hence, it may be inferred that either the spawning site selection at least in some years is less dependent on the temperature, or there have been other factors that have played a stronger role in the latter part of the period. Capelin spawning sites selection could have links to year-class strength and/or timing of stock collapses occurred during the periods 1993–1997 and 2003–2006 (Gjøsæter, 2009). However, since our data does not tell us about how the stocks are spatially distributed, we consider as limiting, any inference based on such direct comparison of stock size.

Similar to the spawning sites, capelin spawning arrival timing has also been hypothesized to be determined by the Barents Sea water temperature (Ozhigin and Luka, 1985). That is, early arrival timing is associated with low temperature and vice versa. We used the inshore ERS data (only catches close to the coast of the spawning regions) to estimate capelin arrival time, which may also be indicative of the spawning time in the respective regions. The ERS data was available only from 2011, with exception of the periods 2016–2017 and 2019–2020 due to the moratorium on capelin fisheries. Capelin approached the coast of the spawning regions in the first two weeks of February. It was only in 2013 when capelin arrived earlier (in late January) (Fig. 6). Although the early capelin arrival in 2013 was associated with the low water temperature in the Barents Sea, the temperature is only relatively low compared with the recent years (Fig. 7). The year 2013 is still considered as a warm year compared to a longer time series (last thirty years). In general, although the recent years 2011–2018 are considered as warming years, the arrival time in several

years was as early as late January - early February. Hence, the arrival time of capelin at the spawning sites may not be solely dependent on the temperature. Fishery fleet behavior is another factor that could potentially affect the arrival time of mature capelin since the date for commencement of commercial fisheries varies among years. On the other hand, once the fisheries open, fishing activities along the whole northern Norwegian coast are relatively concurrent. Hence, it may be argued that there is little potential of fleet behavior impacting the times potential spawners arrive in the spawning regions.

The capelin spawning migration pattern may also be characterized by the capelin fishery pattern along the coasts of the spawning regions. For example, in 2012, the first catch of capelin was on the coast of East Finnmark on the third day of February, then one week later, they were observed (caught) in West Finnmark, and in early March, they arrived in the Troms region. This means that capelin probably approached the spawning regions from the east, and continued moving westward in several groups until they reached the Troms region. On the other hand, in 2011 and 2012, capelin was observed in both East and West Finnmark almost on the same day. This indicates that capelin may have reached Finnmark from two different directions. This corroborates previous findings that in some years, capelin approaches the coast along one route while in others, the capelin may migrate to the coast along two or even three different directions (Gjøsæter, 1998). However, more years with ERS data are required to give a more systematic description of the spawning migration dynamics.

Conclusions

We have developed a method to successfully predict the potential spawning areas of the Barents Sea capelin from the spatial distribution of capelin during scientific surveys in winter. The data in the surveys are not directly linked to spawning, e.g., observations of fish eggs or larvae. Using the ERS data, we were able to estimate the capelin arrival times at the spawning regions. This approach is the best possible for hind-casting capelin spawning grounds from surveys and ERS data. A general observation from our analysis is that there has been a westward extension of the preferred spawning area in the last two decades, regardless of the rising Barents Sea water temperatures. Our goal in a sequel paper will be to obtain a better understanding of this westward expansion by investigating the link between temperature and other physical environmental factors that may influence conditions at the spawning grounds. Furthermore, by integrating the ERS data and winter survey data, we hope to be able to describe the dynamics of capelin spawning migration.

CRediT authorship contribution statement

Salah Alrabeei: Writing – original draft, Methodology, Formal analysis, Software, Visualization. **Sam Subbey:** Conceptualization, Methodology, Writing – review & editing, Supervision. **Sofie Gundersenb:** Data curation, Writing – review & editing. **Harald Gjøsæter:** Writing – review & editing.

Declaration of Competing Interest

The authors declare that they have no known competing financial interests or personal relationships that could have appeared to influence the work reported in this paper.

Appendix A. The spatial distribution of capelin spawning sites

See Figs. A1–A5.

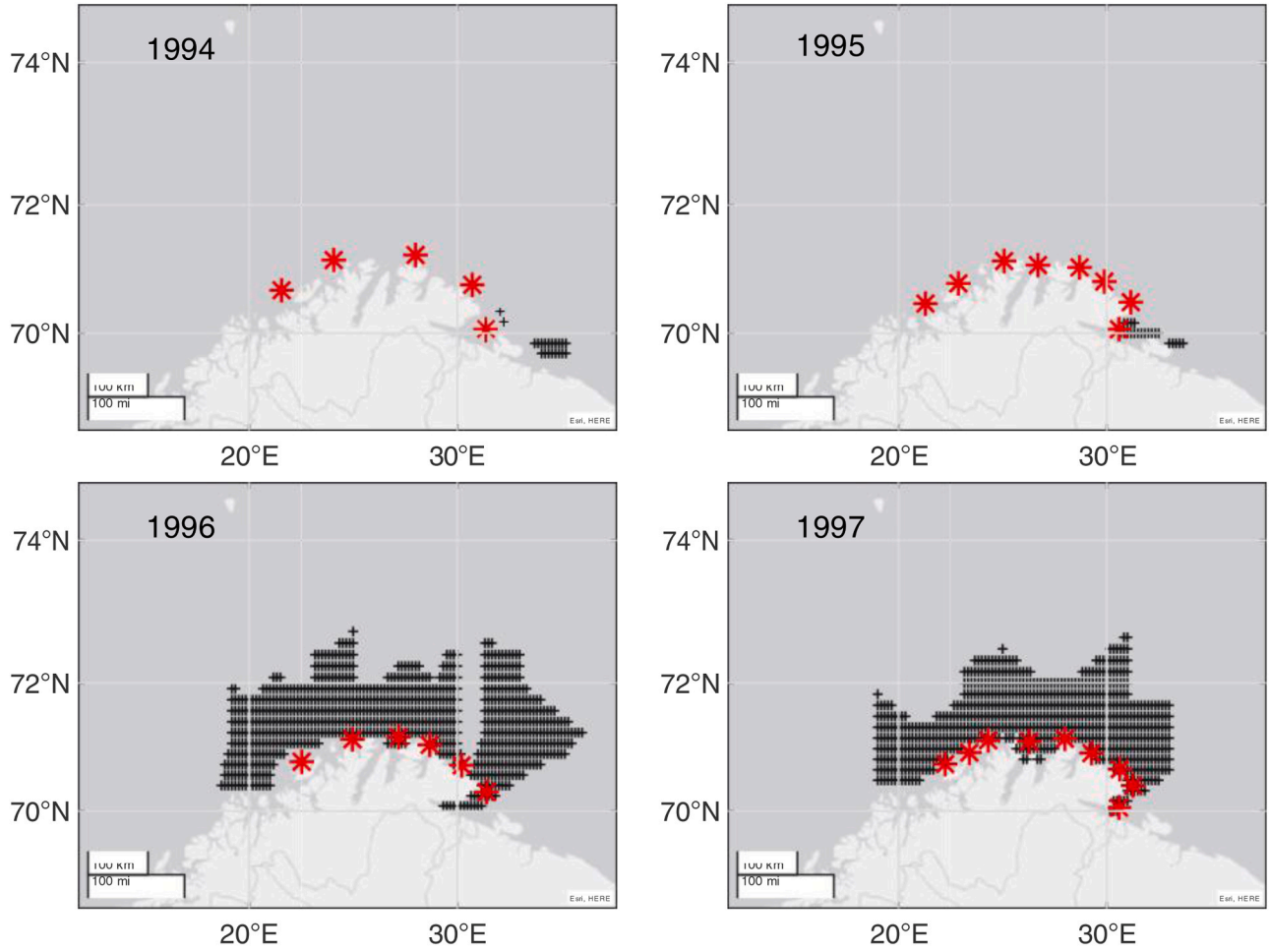

Fig. A1. Predicted spawning sites (red stars) and spring larval distribution (black crosses) during the period 1994–1997. (For interpretation of the references to colour in this figure legend, the reader is referred to the web version of this article.)

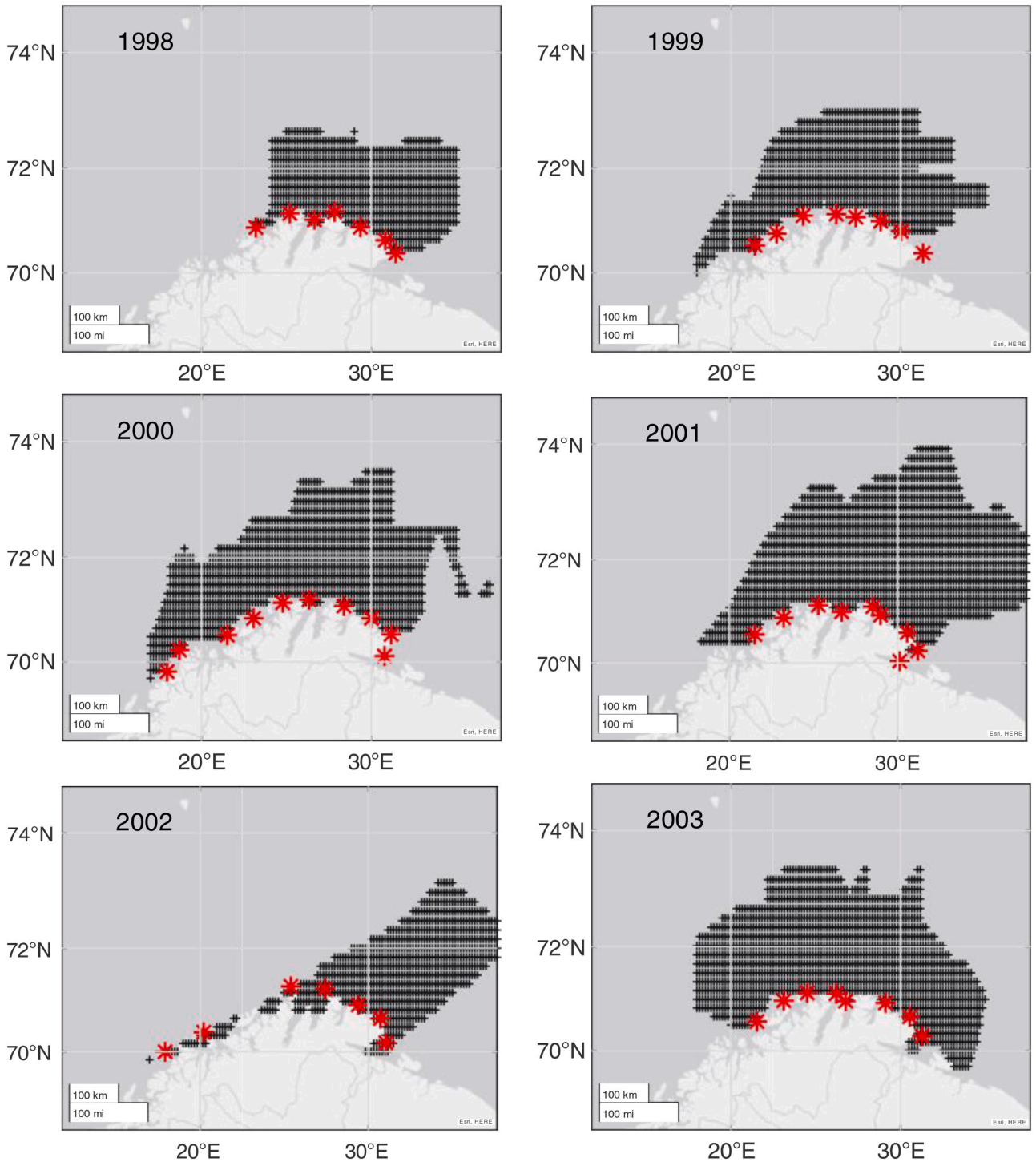

Fig. A2. Predicted spawning sites (red stars) and spring larval distribution (black crosses) during the period 1998–2003. (For interpretation of the references to colour in this figure legend, the reader is referred to the web version of this article.)

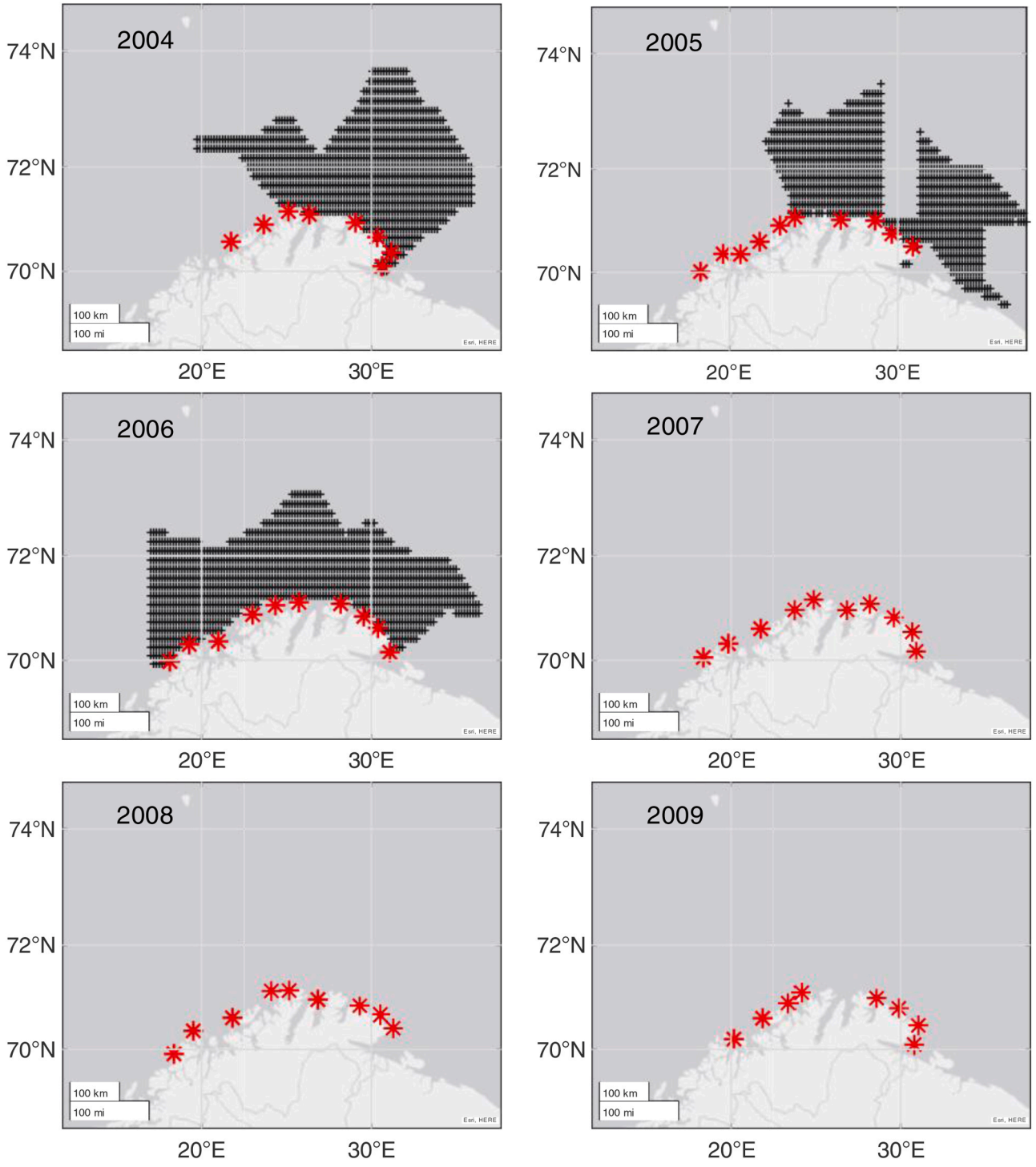

Fig. A3. Predicted spawning sites (red stars) and spring larval distribution (black crosses) during the period 2004–2009. (For interpretation of the references to colour in this figure legend, the reader is referred to the web version of this article.)

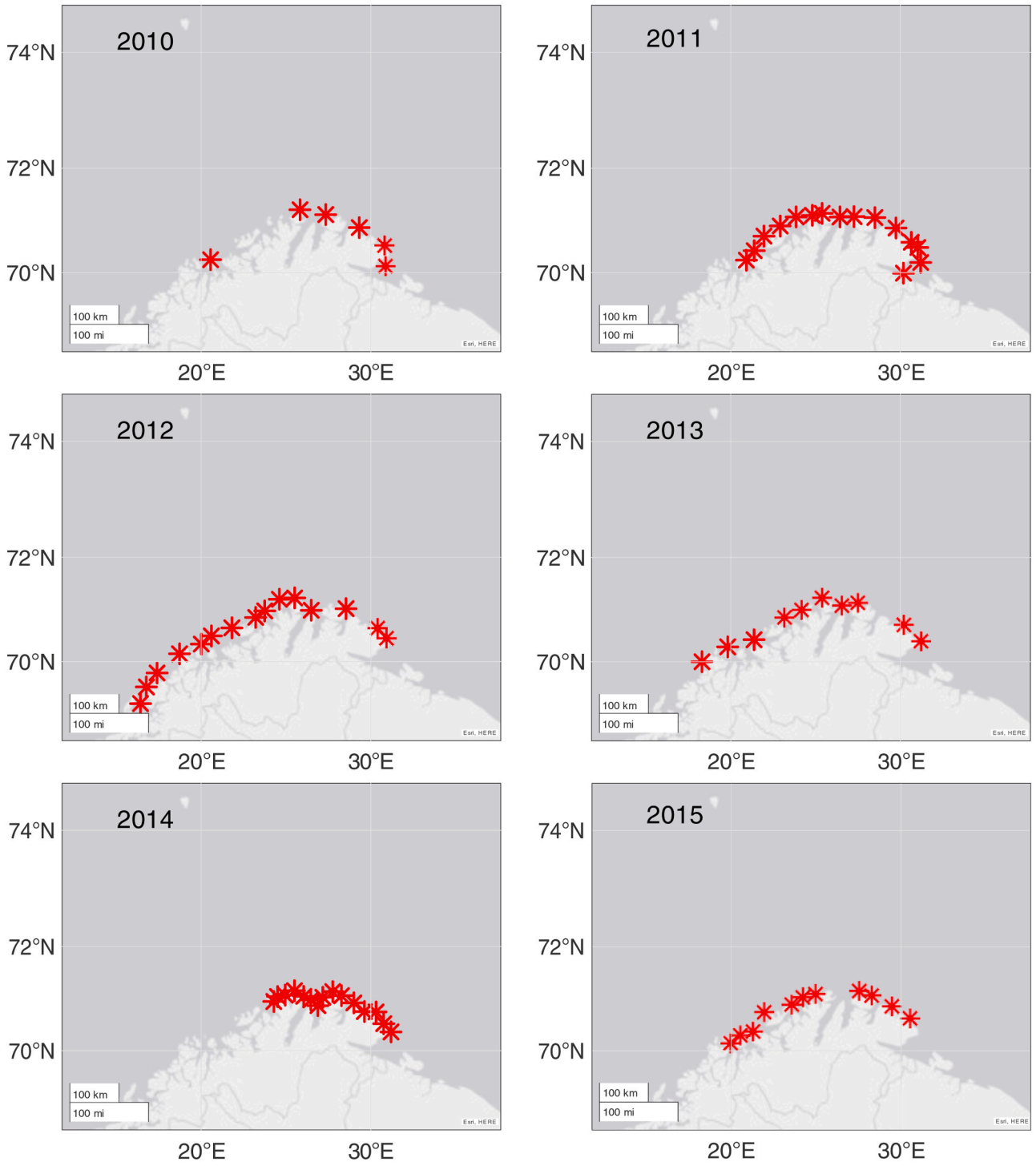

Fig. A4. Predicted spawning sites (red stars) during the period 2010–2015. (For interpretation of the references to colour in this figure legend, the reader is referred to the web version of this article.)

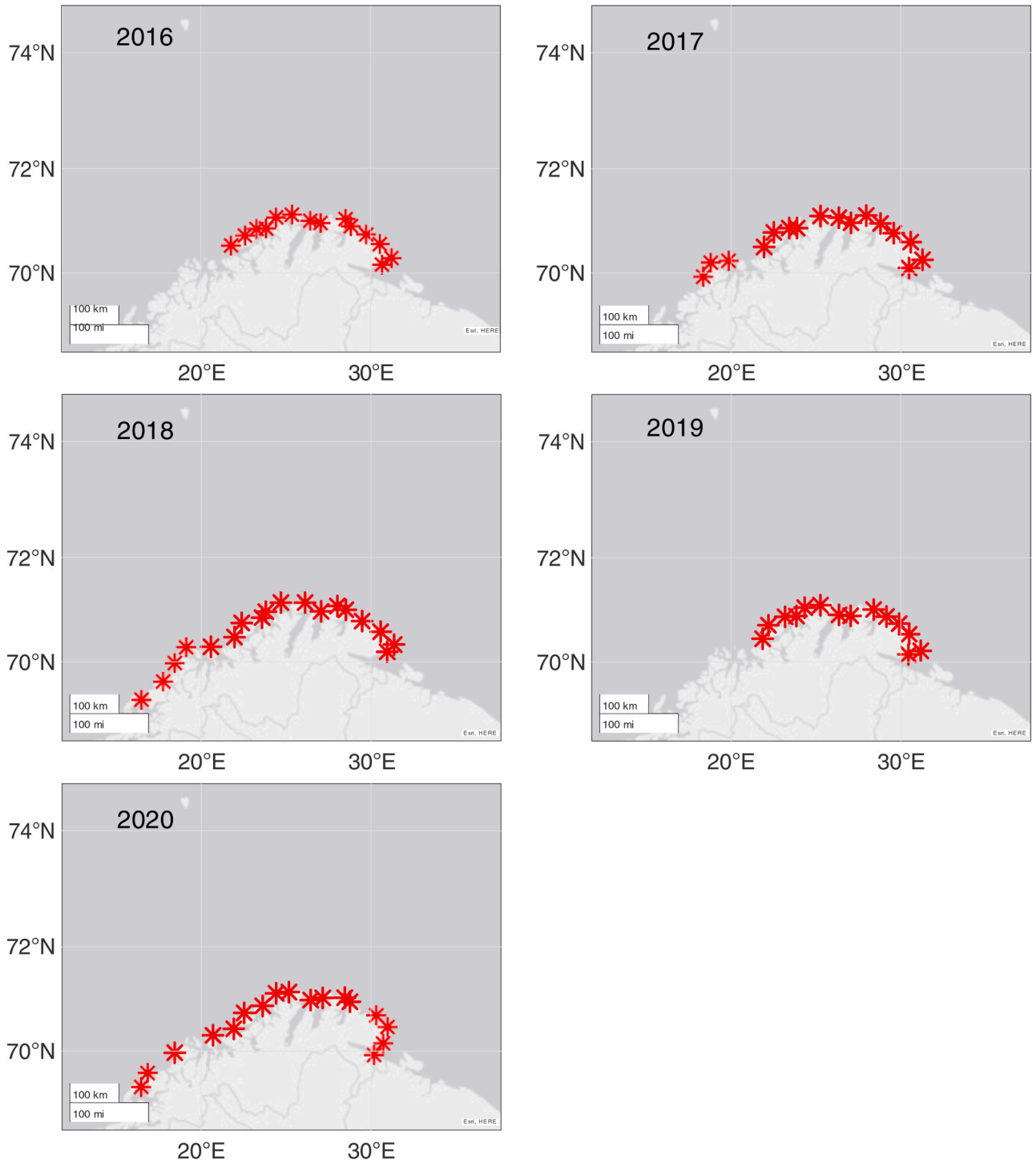

Fig. A5. Predicted spawning sites (red stars) during the period 2016–2020. (For interpretation of the references to colour in this figure legend, the reader is referred to the web version of this article.)

References

Alvheim, O., 1985. Investigations on capelin larvae off northern Norway and in the Barents Sea in 1981–1984. In: Gjøsæter, H. (Ed.), Proceedings of the Soviet-Norwegian Symposium on the Barents Sea Capelin. Institute of Marine Research, Bergen, Norway, pp. 171–184.

Alvheim, O., Dommasnes, A., Martinsen, O., Tjelmeland, S., 1983. Loddeundersøkelser i Barentshavet vinteren 1981. (Capelin investigations in the Barents Sea during the winter 1981). Fisk. Og. Havet 2, 1–10 (In Norwegian with English abstract).

Bakke, S., Bjørke, H., 1973. Diving observations on Barents Sea capelin at the spawning grounds off Northern Norway. Fisk. Skr. Ser. Havunders. 16, 140–147.

Bauer, R., Gräwe, U., Stepputtis, D., Zimmermann, C., Hammer, C., 2014. Identifying the location and importance of spawning sites of Western Baltic herring using a particle backtracking model. ICES J. Mar. Sci. 71, 499–509. https://doi.org/10.1093/icesjms/fst163.

Bez, N., Rivoirard, J., 2001. Transitive geostatistics to characterise spatial aggregations with diffuse limits: an application on mackerel ichtyoplankton. Fish. Res. 50, 41–58. https://doi.org/10.1016/S0165-7836(00)00241-1.

Bidegain, G., Bárcena, J.F., García, A., Juanes, J.A., 2013. LARVAHS: predicting clam larval dispersal and recruitment using habitat suitability-based particle tracking model. Ecol. Model. 268, 78–92. https://doi.org/10.1016/j.ecolmodel.2013.07.020.

Boots, B., Tiefelsdorf, M., 2000. Global and local spatial autocorrelation in bounded regular tessellations. J. Geogr. Syst. 2, 319–348.

Carmack, E., Barber, D., Christensen, J., Macdonald, R., Rudels, B., Sakshaug, E., 2006. Climate variability and physical forcing of the food webs and the carbon budget on panarctic shelves. Prog. Oceanogr. 71, 145–181. https://doi.org/10.1016/j.pocean.2006.10.005.

Carscadden, J., Nakashima, B.S., Frank, K., 1997. Effects of fish length and temperature on the timing of peak spawning in capelin (*Mallotus villosus*). Can. J. Fish. Aquat. Sci. 54, 781–787. https://doi.org/10.1139/f96-331.

Carscadden, J.E., Gjøsæter, H., Vilhjálmsson, H., 2013a. A comparison of recent changes in distribution of capelin (*Mallotus villosus*) in the Barents Sea, around Iceland and in the Northwest Atlantic. Prog. Oceanogr. 114, 64–83. https://doi.org/10.1016/j.pocean.2013.05.005.

Carscadden, J.E., Gjøsæter, H., Vilhjálmsson, H., 2013b. Recruitment in the Barents Sea, Icelandic, and Eastern Newfoundland/Labrador capelin (*Mallotus villosus*) stocks. Prog. Oceanogr. 114, 84–96. https://doi.org/10.1016/j.pocean.2013.05.006.

Christiansen, J.S., Præbel, K., Siikavuopio, S.I., Carscadden, J.E., 2008. Facultative semelparity in capelin *Mallotus villosusI* (Osmeridae)-an experimental test of a life history phenomenon in a sub-arctic fish. J. Exp. Mar. Biol. Ecol. 360, 47–55. https://doi.org/10.1016/j.jembe.2008.04.003.

Dommasnes, A., Hamre, J., 1977. Gyteinnsiget av lodde vinteren 1977. (The spawning migration of capelin during the winter of 1977). Fisk. Og. Havet 1977 3, 1–9 (In Norwegian with English abstract).

Dragesund, O., Gjøsæter, J., Monstad, T., 1973. Estimates of stock size and reproduction of the Barents Sea capelin in 1970-1972. Fisk. Skr. Ser. Havunders. 16, 105–139.

Eriksen, E., 2014.IMR Capelin larvae monitoring, Institute of Marine Research, Norway. ⟨http://ipt.vliz.be/eurobis/resource?r=capelin_larvae⟩.

Erisman, B., Aburto-Oropeza, O., Gonzalez-Abraham, C., Mascareñas-Osorio, I., Moreno-Báez, M., Hastings, P.A., 2012. Spatio-temporal dynamics of a fish spawning aggregation and its fishery in the Gulf of California. Sci. Rep. 2, 1–11. https://doi.org/10.1038/srep00284.

Erisman, B., Heyman, W., Kobara, S., Ezer, T., Pittman, S., Aburto-Oropeza, O., Nemeth, R.S., 2017. Fish spawning aggregations: where well-placed management actions can yield big benefits for fisheries and conservation. Fish Fish 18, 128–144. https://doi.org/10.1111/faf.12132.

Fall, J., Wenneck, T., Bogstad, B., Fuglebakk, E., Gjøsæter, H., Seim, S.E., Skage, M.L., Staby, A., Tranang, C.A., Windsland, K., Russkikh, A.A., Fomin, K., 2020.Fish investigations in the Barents Sea Winter 2020. IMR/PINRO Joint Report Series 2020 2, 1–99.

Gjøsæter, H., 1998. The population biology and exploitation of capelin (*Mallotus villosus*) in the Barents Sea. Sarsia 83, 453–496. https://doi.org/10.1080/00364827.1998.10420445.

Gjøsæter, H., Bogstad, B., Tjelmeland, S., 2002. Assessment methodology for Barents Sea capelin, *Mallotus villosus (Müller)*. ICES J. Mar. Sci. 59, 1086–1095. https://doi.org/10.1006/jmsc.2002.1238.

Gjøsæter, H., Bogstad, B., Tjelmeland, S., 2009. Ecosystem effects of the three capelin stock collapses in the Barents Sea. Mar. Biol. Res. 5, 40–53. https://doi.org/10.1080/17451000802454866.

Gjøsæter, H., Hallfredsson, E.H., Mikkelsen, N., Bogstad, B., Pedersen, T., 2016. Predation on early life stages is decisive for year-class strength in the Barents sea capelin (*Mallotus villosus*) stock. ICES J. Mar. Sci. 73, 182–195. https://doi.org/10.1093/icesjms/fsv177.

Gjøsæter, J., 1972. Recruitment of the Barents Sea capelin 1951-1961. ICES Counc. Meet. 1972/H:24 1–9.

Gjøsæter, J., Sætre, R., Bjørke, H., 1972. Dykkender beiter pÅ loddeegg. (Diving ducks feed on capelin eggs). Sterna 11, 173–176 (In Norwegian).

Hamre, J., 1985. Assessment and management of Barents Sea capelin. In: Gjøsæter, H. (Ed.), Proceedings of the Soviet-Norwegian Symposium on the Barents Sea Capelin. Institute of Marine Research, Bergen, Norway, pp. 5–24.

Hamre, J., Sætre, R., 1976. Gyteinnsiget av lodde vinteren 1976. (The spawning migration of capelin during the winter of 1976). Fisk. Og. Havet 2, 43–51 (In Norwegian with English abstract).

Huse, G., Ellingsen, I., 2008. Capelin migrations and climate change-a modelling analysis. Clim. Change 87, 177–197. https://doi.org/10.1007/s10584-007-9347-z.

ICES, 2019. Report of the Working Group on Integrated Assessments of the Barents Sea (WGIBAR). ICES Sci. Rep. 1, 1–157. https://doi.org/10.17895/ices.pub.5536.

Ingvaldsen, R., Loeng, H., Ottersen, G., Ådlandsvik, B., 2003. Climate variability in the Barents Sea during the 20th century with focus on the 1990s. ICES Mar. Sci. Symp. 160–168.

Ingvaldsen, R.B., Gjøsæter, H., 2013. Responses in spatial distribution of Barents Sea capelin to changes in stock size, ocean temperature and ice cover. Mar. Biol. Res. 9, 867–877. https://doi.org/10.1080/17451000.2013.775450.

Kanungo, T., Mount, D.M., Netanyahu, N.S., Piatko, C.D., Silverman, R., Wu, A.Y., 2002. An efficient k-means clustering algorithm: Analysis and implementation. IEEE Trans. Pattern Anal. Mach. Intell. 24, 881–892. https://doi.org/10.1109/TPAMI.2002.1017616.

Kohonen, T., 1990. The self-organizing map. Proc. IEEE 78, 1464–1480.

Kvile, K.Ø., Fiksen, Ø., Prokopchuk, I., Opdal, A.F., 2017. Coupling survey data with drift model results suggests that local spawning is important for Calanus finmarchicus production in the Barents Sea. J. Mar. Syst. 165, 69–76. https://doi.org/10.1016/j.jmarsys.2016.09.010.

Loeng, H., 1991. Features of the physical oceanographic conditions of the Barents Sea. In: Sakshaug, E., Hopkins, C.C., Øritsland, N.A. (Eds.), Proc. Pro Mare Symp. . Polar Mar. Ecol. 5–18. Trondheim, Norway 12-16 May 1990, Polar Research.

Loeng, H., Nakken, O., Raknes, A., 1983. The distribution of capelin in the Barents Sea in relation to the water temperature in the period 1974-1982. Fisk. Og. Havet, 1983 1, 1–17 (In Norwegian, with English abstract).

Mehl, S., Aglen, A., Bogstad, B., Dingsør, G.E., Gjøsæter, H., Godiksen, J., Johannesen, E., Korsbrekke, K., Murashko, P., Russkikh, A., Staby, A., Wenneck, T.d.L., Wienerroither, R., 2014.Fish investigations in the Barents Sea winter 2013–2014. IMR/PINRO Joint Report Series 2014 2, 1–73.

Monstad, T., Midttun, L., 1973. Loddeundersøkelser med F/F Johan Hjort i Barentshavet i Januar-Februar 1973. (Capelin investigations with R/V Johan Hjort in January-February 1973). Fisk. Gang 59, 817–821 (In Norwegian with English abstract).

Ozhigin, V., Luka, G., 1985. Some peculiarities of capelin migrations depending on thermal conditions in the Barents Sea, in: Gjøsæter, H. (Ed.), Proceedings of the Soviet-Norwegian Symposium on the Barents Sea Capelin. Institute of Marine Research, Bergen, Norway, 1985, 135–147.

Ozhigin, V., Ushakov, N., 1985. The effect of the thermal conditions of the Sea and atmospheric circulation on the distribution of the Barents Sea capelin feeding areas, in: Gjøsæter, H. (Ed.), Proceedings of the Soviet-Norwegian Symposium on the Barents Sea Capelin. Institute of Marine Research, Bergen, Norway, 1985, 149–156.

Petitgas, P., Secor, D.H., McQuinn, I., Huse, G., Lo, N., 2010. Stock collapses and their recovery: mechanisms that establish and maintain life-cycle closure in space and time. ICES J. Mar. Sci. 67, 1841–1848. https://doi.org/10.1093/icesjms/fsq082.

Sadovy, Y., Domeier, M., 2005. Are aggregation-fisheries sustainable? Reef fish fisheries as a case study. Coral Reefs 24, 254–262. https://doi.org/10.1007/s00338-005-0474-6.

Sætre, R., Gjøsæter, J., 1975. Ecological investigations on the spawning grounds of the Barents Sea capelin. Fisk. Skr. Ser. Havunders. 16, 203–227.

Singh, W., Bárðarson, W., Jónsson, S.Þ., Elvarsson, B., Pampoulie, C., 2020. When logbooks show the path: Analyzing the route and timing of capelin (Mallotus villosus) migration over a quarter century using catch data. Fish. Res. 230. https://doi.org/10.1016/j.fishres.2020.105653.

Skaret, G., Peña, H., Totland, A., Anthonypillai, V., Karlson, S., Drivenes, L., Røttingen, J., Bogetveit, F., 2020.Testing of trawl-acoustic stock estimation of spawning capelin 2020. Institute of Marine Research, Norway, Cruise Report No 2, 1–47.

Tanemura, M., Ogawa, T., Ogita, N., 1983. A new algorithm for three-dimensional Voronoi tessellation. J. Comput. Phys. 51, 191–207.

Tobin, A., Currey, L., Simpfendorfer, C., 2013. Informing the vulnerability of species to spawning aggregation fishing using commercial catch data. Fish. Res. 143, 47–56. https://doi.org/10.1016/j.fishres.2013.01.011.

Ushakov, N., Ozhigin, V., 1987. The abundance of year classes of the Barents Sea Capelin and peculiarities of the distribution of the young in relation to hydrographic conditions. In: Loeng, H. (Ed.), Proc. Third Sov. -Nor. Synposium 159–167. Murmansk, 26-28 May 1986. Institute of Marine Research, Bergen 1987.

Vitale, F., Börjesson, P., Svedäng, H., Casini, M., 2008. The spatial distribution of cod (*Gadus morhua L.*) spawning grounds in the Kattegat, eastern North Sea. Fish. Res. 90, 36–44. https://doi.org/10.1016/j.fishres.2007.09.023.

Woillez, M., Rivoirard, J., Petitgas, P., 2009. Notes on survey-based spatial indicators for monitoring fish populations. Aquat. Living Resour. 22, 155–164. https://doi.org/10.1051/alr/2009017.